2.3 A NEW GENERATION OF ANGULAR DISTRIBUTION MODELS FOR TOP-OF-ATMOSPHERE RADIATIVE FLUX ESTIMATION FROM THE CLOUDS AND THE EARTH'S RADIANT ENERGY SYSTEM (CERES) SATELLITE INSTRUMENT

N. G. Loeb[1*], N. Manalo-Smith[2], K. Loukachine[3], S. Kato[1], B. A. Wielicki[4]

[1]Hampton University, Hampton, VA
[2]Analytical Services and Materials, Inc., Hampton, VA
[3]Science Application International Corporation, Hampton, VA
[4]NASA Langley Research Center, Hampton, VA

1. INTRODUCTION

The Clouds and the Earth's Radiant Energy System (CERES) investigates the critical role that clouds and aerosols play in modulating the radiative energy flow within the Earth-atmosphere system (Wielicki et al., 1995). CERES builds upon the foundation laid by previous missions such as the Earth Radiation Budget Experiment (ERBE) (Barkstrom, 1984) to provide highly accurate top-of-atmosphere (TOA) radiative fluxes together with coincident cloud and aerosol properties inferred from high-resolution imager measurements (e.g. VIRS, MODIS). The CERES instrument measures radiances in three channels: a shortwave channel to measure reflected sunlight, a window channel to measure Earth-emitted thermal radiation in the 8-12 μm "window" region, and a total channel to measure wavelengths between 0.3 and 200 μm. After removing the influence of instrument spectral response from the measurements, CERES radiances are converted to reflected shortwave (SW), emitted longwave (LW) and emitted window (WN) TOA radiative fluxes. The radiance-to-flux conversion involves applying scene-dependent empirical Angular Distribution Models (ADMs) constructed from several months of CERES data. This paper presents an overview of the methodology used to construct and validate new CERES ADMs from the Tropical Rainfall Measuring Mission (TRMM) satellite. A separate set of ADMs are currently under development for CERES/Terra.

2. OBSERVATIONS

CERES/TRMM was launched on November 27, 1997 in a 350-km circular, precessing orbit with a 35° inclination angle. TRMM has a 46-day repeat cycle, so that a full range of solar zenith angles over a region are acquired every 46 days. On TRMM, CERES has a spatial resolution of approximately 10 km (equivalent diameter) and operates in three scan modes: cross-track, along-track, and rotating azimuth plane (RAP) mode. In RAP mode, the instrument scans in elevation as it rotates in azimuth, thus acquiring radiance measurements from a wide range of viewing configurations. The CERES instrument on TRMM was shown to provide an unprecedented level of calibration stability (≈0.25%) between in-orbit and ground calibration (Priestley et al., 1999). Unfortunately, the CERES/TRMM instrument suffered a voltage converter anomaly and only acquired 9 months of science data.

All nine months of the CERES/TRMM Single Scanner Footprint TOA/Surface Fluxes and Clouds (SSF) product between 40°S-40°N from January-August 1998, and March 2000, are considered. The CERES SSF product combines CERES radiances and fluxes with scene identification information inferred from coincident high spatial and spectral resolution Visible Infrared Scanner (VIRS) measurements (Kummerow et al., 1998), and meteorological fields based on European Centre for Medium-Range Weather Forecasts (ECMWF) data assimilation analysis (Rabier et al, 1998). A comprehensive description of all parameters appearing in the CERES SSF is provided in the CERES Collection Guide (Geier et al., 2001). During the 9 months of CERES data acquisition, SSFs were produced for 269 days. CERES was in crosstrack mode for 192 days, RAP mode for 68 days and alongtrack mode for 9 days.

TOA fluxes from the SSF are compared with those from the CERES "ERBE-Like" product. The CERES ERBE-like product is produced in order to extend the historical record of Earth radiation budget observations, by processing CERES measurements with algorithms developed during ERBE (Smith et al., 1986).

3. CERES ADMs

TOA flux is the radiant energy emitted or scattered by the Earth-atmosphere per unit area. Flux is related to radiance (I) as follows:

$$F(\theta_o) = \int_0^{2\pi} \int_0^{\pi/2} I(\theta_o, \theta, \phi) \cos\theta \sin\theta \, d\theta d\phi \qquad (1)$$

where θ_o is the solar zenith angle, θ is the observer viewing zenith angle and ϕ is the relative azimuth angle defining the azimuth angle position of the observer relative to the solar plane. An ADM is a function that provides anisotropic factors (R) to determine the TOA flux from an observed radiance as follows:

*Corresponding author address: Norman G. Loeb, Mail Stop 420, NASA Langley Research Center, Hampton, VA 23681-2199; e-mail: n.g.loeb@larc.nasa.gov

$$F(\theta_o) = \frac{\pi I(\theta_o, \theta, \phi)}{R(\theta_o, \theta, \phi)} \quad (2)$$

CERES TOA fluxes are defined at the 20-km reference level since this level has been shown to be the most appropriate for radiation budget studies (Loeb et al., 2002a).

Because CERES measures only part of the upwelling radiation from a scene at any given time from one or more angles, *F* (or *R*) cannot be measured instantaneously. Instead, *R* is estimated from a set of pre-determined empirical ADMs defined for several scene types with distinct anisotropic characteristics. Each ADM is constructed from a large ensemble of radiance measurements that are sorted by scene type and viewing geometry. The ADM anisotropic factors for a given scene type (*j*) are given by:

$$R_j(\theta_{oi}, \theta_k, \phi_l) = \frac{\pi \bar{I}_j(\theta_{oi}, \theta_k, \phi_l)}{F_j(\theta_{oi})} \quad (3)$$

where $\bar{I}_j$ is the average radiance (corrected for Earth-sun distance in the SW) of all measurements with scene type *j* lying in angular bin $(\theta_{oi}, \theta_k, \phi_l)$, and F_j is the upwelling flux derived from $\bar{I}_j$ and radiance contributions from slant paths above the Earth's tangent point (Loeb et al., 2002a).

CERES ADM scene types are defined according to imager-derived cloud and ECMWF meteorological parameters that have a strong influence on the anisotropy (or angular variation) of the radiance field. In the SW, the primary scene type parameters are surface type, cloud fraction, cloud phase and cloud optical depth. In the LW and WN channels, ADM scene types are defined by surface type, precipitable water content, cloud fraction, lapse rate (clear scenes), surface-cloud temperature difference and cloud emissivity. Several hundred ADM scene types are defined for different combinations of these parameters (Loeb et al., 2002b). This approach is a major advance over ERBE, which used coarse-resolution broadband SW and LW radiances to define ADMs for only 12 scene types (Suttles et al., 1988) stratified by surface type and four approximate cloud cover classes (clear, partly cloudy, mostly cloudy and overcast) (Wielicki and Green, 1989).

Fig. 1 shows an example of SW CERES ADMs for thin and thick overcast ice clouds with θ_o=50°-60°. For the thin cloud case, the anisotropic factor ranges from 0.6 to 3.3, compared to 0.9 to 1.6 for the thick cloud case. The largest sensitivity to cloud optical depth occurs at near-nadir views, where the anisotropic factor changes by 50%. Examples of LW and WN ADMs over clear land are provided in Manalo-Smith et al. (2002).

4. TOA FLUX COMPARISONS

To demonstrate the differences between SW TOA fluxes from the ERBE ADMs and the new CERES/TRMM ADMs, Fig. 2 shows SW TOA flux differences as a function of cloud optical depth for overcast liquid water clouds (Fig. 2a) and ice clouds (Fig. 2b). At small cloud optical depths, the ERBE SW TOA fluxes are smaller than the SSF fluxes determined using the new CERES/TRMM ADMs by up to 75 W m^{-2}, while differences of the same magnitude but of opposite sign occur for large cloud optical depths. The reason is because ERBE only has one overcast ADM, while CERES/TRMM ADMs define 14 models to account for the variations in SW radiance anisotropy with cloud optical depth. For thin clouds, the ERBE models underestimate the anisotropy, while they overestimate the anisotropy for thick clouds.

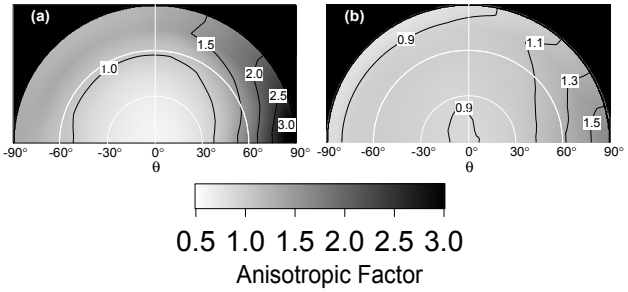

Fig. 1 Overcast ice cloud ADMs with cloud optical depths between (a) 1.0-2.5 and (b) 20-25 for θ_o=50°-60°.

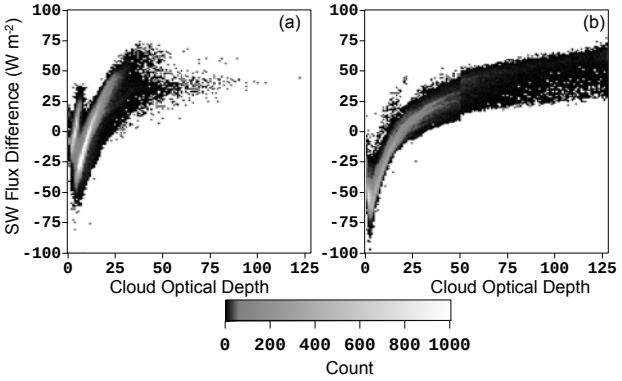

Fig. 2 SW flux difference (CERES ERBE-Like minus CERES SSF) against cloud optical depth over ocean for θ_o=42° - 44° and θ< 25°. (a) Liquid water clouds; (b) Ice clouds.

A powerful validation tool for assessing TOA flux consistency is to examine whether ADM-derived TOA fluxes or albedos exhibit any dependence on viewing geometry. Fig. 3a-b show ERBE-Like and CERES/TRMM all-sky mean TOA albedos stratified by viewing zenith angle and relative azimuth angle for θ_o=40°-50°. The gray line corresponds to the albedo determined by directly integrating the radiances (Eq. (1)) and converting flux to albedo. The ERBE-Like albedos (Fig. 3a) show a systematic relative increase of 10%

from nadir to the limb. TOA albedos are underestimated close to nadir, and overestimated at large viewing zenith angles, especially for ϕ=0°-10°. In contrast, CERES/TRMM albedos show little dependence on viewing geometry and generally remain within a few percent of the direct integration albedo. Loukachine et al. (2002) show that ERBE-Like LW TOA fluxes systematically decrease by 3.5% (or 9 W m^{-2}) from nadir to the limb, while fluxes based on the CERES/TRMM ADMs vary by < 0.7% (< 2 W m^{-2}).

The multiangle capability of CERES can also be used to estimate uncertainties in instantaneous TOA flux and albedo estimates. Fig. 4 shows relative frequency distributions of multiangle albedo dispersion over clear ocean for CERES SSF, ERBE-Like, and by assuming each scene is Lambertian. The multiangle dispersion is determined by collocating coincident alongtrack TOA albedo estimates over 30-km clear ocean target areas and calculating the standard deviation-to-mean albedo ratio for each target area. Nine alongtrack days are considered. If the clear ocean scenes are approximately spatially homogeneous over the 30-km target areas, the albedo dispersion should be close to zero, since TOA flux should be independent of viewing geometry. Fig. 4 shows that TOA albedos based on the new CERES/TRMM ADMs used in the CERES SSF product have a much smaller dispersion compared to TOA fluxes from the ERBE-Like product. On average, the multiangle TOA albedo dispersion is 2.2% for SSF, 8.8% for ERBE-Like, and 17% for the Lambertian assumption.

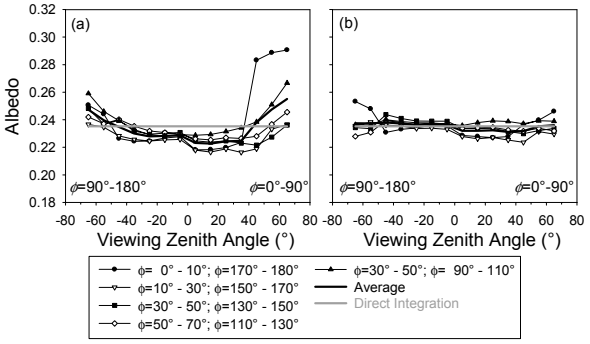

Fig. 3 All-sky mean albedo against viewing zenith angle and relative azimuth angle for θ_o=40°-50°. (a) ERBE-Like; (b) CERES/TRMM.

Uncertainties in regional mean TOA fluxes are estimated by comparing ADM-derived TOA flux estimates with fluxes evaluated by direct integration of the radiances over 20°×20° latitude/longitude boxes in the SW, and 10°×10° latitude/longitude boxes in the LW. The SW results correspond to 24-hour averages for a March solar irradiance distribution. To quantify how ADM errors affect gridded time-averaged TOA fluxes (Young et al., 1998), the mean ADM flux biases in different angular bins are weighted by a factor that accounts for the relative influence of satellite viewing geometry on gridded time-averaged fluxes. Because CERES has a fixed scan rate, more weight is assigned to flux biases at the larger viewing zenith angles (e.g. θ=70°). Table 1 shows the regional mean flux bias (Δ) and root-mean-square (*RMS*) error when CERES footprints with θ < 50° and θ < 70° are considered. When θ < 50°, the ERBE-Like ADMs underestimate the direct integration TOA SW flux by 2.73 W m^{-2}, and overestimate the LW flux by 4.35 W m^{-2}. For θ < 70°, ERBE-Like SW and LW flux biases are reduced to 0.43 W m^{-2} and 1.22 W m^{-2}, respectively. This large reduction is due to compensating errors at large and small viewing zenith angles. In contrast, the SSF TOA flux biases are near zero in the SW for both θ ranges, and remain < 1 W m^{-2} in the LW. Flux *RMS* errors in Table 1 show that regional TOA flux accuracy from the SSF is improved by a factor of 1.5-2 in the SW and a factor of 3 in the LW relative to ERBE-like.

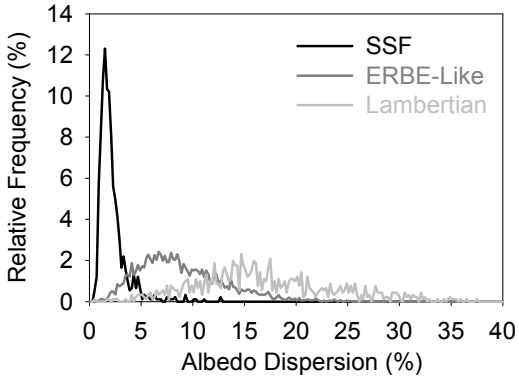

Fig. 4 Relative frequency of multiangle albedo dispersion over clear ocean based on CERES SSF, ERBE-Like and Lambertian albedo estimates.

Table 1 Monthly mean regional SW and LW TOA flux bias and *RMS* error (W m^{-2}) for ERBE-Like and SSF TOA fluxes as a function of viewing zenith angle range.

	SW			
	ERBE-Like		SSF	
θ-range	Δ	*RMS*	Δ	*RMS*
θ < 50°	-2.73	3.12	0.03	1.42
θ < 70°	0.43	0.82	-0.06	0.51
	LW			
	ERBE-Like		SSF	
θ-range	Δ	*RMS*	Δ	*RMS*
θ < 50°	4.35	4.60	0.87	1.62
θ < 70°	1.22	1.33	0.29	0.49

5. SUMMARY

The CERES experiment will provide global broadband TOA radiative fluxes in the SW, LW and WN regions together with coincident imager-derived cloud and aerosol properties and atmospheric state parameters from 4-D assimilation products. One of the

major advances in CERES is the availability of improved ADMs for estimating TOA radiative fluxes from broadband radiance measurements. Multiangle CERES measurements and coincident imager cloud information are used to construct empirical ADMs for scene types defined by parameters that have a strong influence on the anisotropy (or angular dependence) of TOA radiances. At the present time, a complete set of ADMs are available for the CERES instrument on TRMM. The CERES/TRMM ADMs are available for viewing and downloading at the following web address: http://asd-www.larc.nasa.gov/Inversion/. A set of global ADMs are under development based on CERES and MODIS observations on Terra (and eventually, Aqua).

The advantages of combining CERES and imager data are demonstrated by comparing TOA fluxes from the CERES SSF and ERBE-Like products. The CERES SSF product uses the new CERES ADMs, whereas fluxes on the ERBE-Like product are based on ADMs developed during the ERBE experiment for only 12 scene types. When SSF and ERBE-like fluxes are stratified by scene type parameters that have a strong influence on anisotropy (e.g. cloud optical depth), systematic SW flux biases of up to 75 W m-2 (for θ_o=42°-44°) are observed for overcast ice clouds. All-sky mean fluxes from the new CERES ADMs are shown to be consistent to within 2% in the SW, and 0.7% (or 2 W m^{-2}) in the LW. In contrast, ERBE-Like mean fluxes show a systematic dependence on viewing zenith angle of 10% in the SW, and 3.5% (or 9 W m^{-2}) in the LW. Multiangle consistency checks show that instantaneous flux errors from the new CERES ADMs are smaller than those from the ERBE ADMs by up to a factor of 4 for clear ocean scenes. Regional TOA flux accuracy from the CERES SSF is improved by a factor of 2-3 improvement compared to CERES ERBE-Like flux accuracy.

6. REFERENCES

Barkstrom, B.R., 1984: The Earth Radiation Budget Experiment (ERBE), *Bull. Amer. Meteorol. Soc.*, **65**, 1170-1186.

Geier, E.B., et al., Single satellite footprint TOA/Surface fluxes and clouds (SSF) collection document, [available on-line from http://asd-www.larc.nasa.gov/ceres/ASDceres.html], 2001.

Kummerow, C., W. Barnes, T. Kozu, J. Shiue, and J. Simpson, 1998: The Tropical Rainfall Measuring Mission (TRMM) sensor package, *J. Atmos. Ocean. Tech.*, **15**, 809-817.

Loeb, N.G., S. Kato, and B.A. Wielicki, 2002a: Defining top-of-atmosphere flux reference level for Earth radiation budget studies, *J. Climate*, (accepted).

Loeb, N.G., et al., 2002b: Angular distribution models for top-of-atmosphere radiative flux estimation from the Clouds and the Earth's Radiant Energy System Instrument on the Tropical Rainfall Measuring Mission Satellite. Part I: Methodology, *J. Appl. Meteor.*, submitted, 2002.

Loukachine, K., N.G. Loeb, and N. Manalo-Smith, 2002: Validation of top-of-atmosphere radiative flux estimates from the Clouds and the Earth's Radiant Energy System (CERES) Angular Distribution Models. *11th Conference on Atmospheric Radiation*, Ogden, Utah.

Manalo-Smith, N., N.G. Loeb, and K. Loukachine, 2002: Development of longwave and window angular distribution models from the Clouds and the Earth's Radiant Energy System (CERES) experiment, *11th Conference on Atmospheric Radiation*, Ogden, Utah.

Priestley K.J., et al., 1999: Radiometric performance of the Clouds and the Earth's Radiant Energy System (CERES) proto-flight model on the Tropical Rainfall Measuring Mission (TRMM) spacecraft for 1998, *Proc. AMS 10th Conf. Atmos. Rad.*, Madison, WI, 33-36, June 28-July 2.

Rabier, F., J.-N. Thepaut, and P. Courtier, 1998: Extended assimilation and forecast experiments with a four-dimensional variational assimilation, *Quart. J. Roy. Meteor. Soc.*, **124**, 1861-1887.

Smith, G.L., et al., 1986: Inversion methods for satellite studies of the earth radiation budget: Development of algorithms for the ERBE mission, *Rev. Geophys.,* **24**, 407–421.

Suttles, J.T., et al., 1988: Angular radiation models for Earth-atmosphere systems, Vol. I–shortwave radiation, *Rep. NASA RP-1184*, NASA, Washington, D.C., 1988.

Wielicki, B.A., et al., 1995: Mission to planet Earth: Role of clouds and radiation in climate,. *Bull. Amer. Meteor. Soc.*, **76**, 2125-2153.

Wielicki, B.A., and R.N. Green, 1989: Cloud identification for ERBE radiation flux retrieval, *J. Appl. Meteor.*, **28**, 1133-1146.

Young, D.F., et al., 1998: Temporal interpolation methods for the Clouds and the Earth's Radiant Energy System (CERES) experiment, *J. Appl. Meteor.*, **37**, 572-590.